

Preliminary Results of the Noiseless Preflash Test (prop. 8450)

A.B. Schultz, I. Heyer, and J. Biretta
December 16, 1999

ABSTRACT

We report preliminary results from analysis of the WFPC2 noiseless preflash test data (program ID: 8450). The short 16 sec. exposures were analyzed for this report. (The long exposure observations of 80 sec. and 400 sec. were lost due to guide star reacquisition failure, HOPR 587 was filed against 8450, and a repeat has been approved.) The calibration lamp was used to preflash the wide field CCDs to about 2000 counts, and the preflash was read out before the start of the science observations. In principle, this might fill the CCD traps while introducing no noise in the science image (i.e. noiseless). Stars within the globular cluster Omega Cen (HD116790, NGC 5139) were positioned in the WF4, WF3, and WF2 apertures. Photometry of faint star images showed on average a 3.0 +/- 0.9% enhancement in the stellar counts (at Y=800) in the preflash exposures. This is consistent with the noiseless preflash giving only a partial reduction in CTE. The majority of the CTE effect must be due to traps which release their charge on time scales of less than two minutes.

1. Introduction

WFPC2 Charge-Coupled Devices (CCDs) have a charge transfer efficiency (CTE) problem (ISR-97-05, ISR-97-08, TIR-98-01, ISR-98-02). CTE is a factor that measures the loss of electrons during transfer from one pixel to the next pixel. The measured CTE for the WFPC2 CCDs detectors is under certain conditions ~0.99995 reading down a column. A target will appear to be fainter when observed at the top of the CCD (Y=800) compared to photometry obtained when the target is positioned at the bottom of the CCD (Y=1). This is due to a loss of charge during the transfer from one potential well to the next. This is a serious problem for photometry of faint sources (< 500 counts).

The WFPC2 CCDs were manufactured by Loral (formerly Ford Aerospace). The CCDs are thick, front side illuminated devices with a Lumogen phosphor coating. The

design and fabrication are based on the TI 800X800 format which were used for the WFPC1 CCDs. The WFPC2 CCDs are operated at a temperature of -88°C .¹

Incident light on the CCDs will create electron-hole pairs; the electrons migrate to the potential wells (pixels) where they are stored and accumulated during an exposure. During readout these charge packets are shifted (transferred) vertically through adjacent wells by changing the bias of each well by clocking. The charge packets are clocked vertically to the horizontal shift register. The output of the horizontal shift register is connected to a pre-amplifier which converts the charge into a voltage signal. Ideally, the CTE is very high for CCDs and the loss of charge due to clocking through the material is extremely small. The WFPC2 CCDs exhibit a less than ideal CTE.

2. CCD traps

Bulk traps in CCDs are electrically active regions due to defects in the crystalline silicon. They are related to impurities and imperfections in the silicon material. As charge packets are transferred through the device, charge is lost to all empty traps in the material. Bulk traps are active at all operating temperatures.

Janesick et al. (1990) report laboratory studies for ionizing radiation effects on CCDs and present a model (The CCD Radiation Transfer Model) for predicting radiation damage effects in CCDs. They show that high energy incident radiation can create silicon vacancies and ionization damage by the passage of particles through the material. High energy protons can displace silicon atoms from their lattice positions by coulombic or nuclear collision. Displacement of silicon atoms can create trapping sites in the CCD's signal channel which degrades CTE. These silicon vacancies typically migrate to and get trapped near impurity atoms. Janesick et al. indicate that radiation induced traps begin to freeze out (become inactive) at -50°C and become inactive at -100°C . Their study indicates that at very low temperatures ($< -100^{\circ}\text{C}$), once an electron fills the proton trap, the trap will remain filled due to the long emission time constant, and CTE improves.

In principle, poor CTE at low light levels (i.e., loss of charge due to traps) can be prevented by filling the traps before reading out the CCD. The CCD can be preflashed by a light source, such as the calibration lamp for WFPC2, to provide a pedestal of charge to fill the traps. This induced pedestal is sometimes called a "fat zero". Once traps are filled, the lifetime to remain filled is of fundamental importance.

Biretta and Mutchler (1998) suggested a modification of this method where the pre-flash is exposed and read out prior to the science exposure. They observed that targets could leave residual images lasting tens of minutes, and hypothesized that these were caused by the traps responsible for CTE. Reading out the preflash would leave the traps

1. Clampin, M. 1992, WFPC-II CCDs, WFPC2-ISR-1992-006.

filled while contributing no extra noise to the science image, hence the term “noiseless” preflash.

3. Commanding a WFPC2 exposure

Preflashing the CCD chip should fill most of the charge traps before they can affect the following science observation. The question that needs to be addressed is: “What is the time scale(s) for the electrons to diffuse out of the traps?”

WFPC2 CCDs are commanded to be in autoflush mode except during exposures, and are turned off during South Atlantic Anomaly (SAA) passages. The continuous clocking of WFPC2 CCDs will flush charge from the traps and limit the usefulness of preflashing to exposure sequences where the calibration lamp is turned on just prior to the science exposure.

The timing sequence for turning on the calibration lamp and the execution of the subsequent science observation is critical to the success of preflashing. Table 1 presents the timing sequence for the 8450 observations. No filter change occurred as the flat field and the science observations were obtained using the F555W filter. Nor was there an alignment change (pointing change) between the flat field and the science observations.

Table 1. WFPC2 Commanding Timing Sequence (program ID: 8450).

exposure	commanding time (min./sec.)	Comments
preflash	0:00	start detector flush
	0:16.4	lamp on/open shutter
	0:46.4	close shutter/lamp off
	1:00	start readout
	1:52	end readout
target	2:00	start detector flush
	2:16.4	open shutter
	2:32.4	close shutter
	3:00	start readout
	3:52	end readout

The start of the WFPC2 readout is timed to the next Major Frame Pulse (MFP) which is close to the start of the next minute. Observations that complete before the start of the next MFP are held on the CCDs until the next MFP. All commanding times are from the STScI Commanding Group.

4. Observations

The globular cluster Omega Cen (HD116790) was observed on July 28 1999 (program ID: 8450). The globular cluster was observed before and after a preflash (30 sec. INTFLAT lamp exposure). Each observational sequence started with two darks followed by target, preflash, and target observations. The dark observations should have removed any residual charge from the CCD arrays from prior exposures. The INTFLAT observations were read out (i.e. noiseless) prior to the start of the science observations. The short exposures (16 sec.) with the target positioned in WF4, WF3, and WF2 were analyzed for this report.

Table 2 presents the three sets of short 16 sec. exposures that were reduced and analyzed for this study. Due to the critical time dependence of the preflash, the UT start times (TIME-OBS) of the observations are listed in the table.

Table 2. WFPC2 CAL Program 8450 Visit 01, Noiseless Preflash Test, F555W filter.

Orbit	LINENUM	APERTURE	Obs.	TIME-OBS	Comments
1	10	WFALL	u5ka0101r	13:40:13	dark, exp=1800 sec.
			u5ka0102r	14:12:13	dark, exp=1800 sec.
2	11	WF4	u5ka0103r	15:08:13	Omega Cen
			u5ka0104r	15:10:13	“
	12	WF4	u5ka0105r	15:13:13	INTFLAT, exp=30 sec.
	13	WF4	u5ka0106r	15:15:13	Omega Cen
u5ka0107r			15:17:13	“	
3	20	WFALL	u5ka0108r	15:23:13	dark, exp=1800 sec.
			u5ka0109r	15:55:13	dark, exp=1800 sec.
	21	WF3	u5ka010ar	16:44:13	Omega Cen
			u5ka010br	16:46:13	“
22	WF3	u5ka010cr	16:49:13	INTFLAT, exp=30 sec.	
		23	WF3	u5ka010dr	16:51:13
	u5ka010er	16:53:13		“	
30	WFALL	u5ka010fr	16:59:13	dark, exp=1800 sec.	
		u5ka010gr	17:31:13	dark,exp=1800 sec.	
4	031	WF2	u5ka010hr	18:06:13	Omega Cen
		WF2	u5ka010ir	18:08:13	“

Orbit	LINENUM	APERTURE	Obs.	TIME-OBS	Comments
	032	WF2	u5ka010jr	18:11:13	INTFLAT,exp=30 sec.
	033	WF2	u5ka010kr	18:13:13	Omega Cen
		WF2	u5ka010lr	18:15:13	'

Three out of four guide star REACQs (re-acquisitions) failed, resulting in the loss of the long 400 second exposures. One set of the WF2 short (16 sec.) and medium (80 sec.) exposures were obtained on gyros, and the star 80 sec. exposure images are trailed. HOPR 587 was filed against 8450 and a repeat was approved. All observations were obtained in consecutive orbits.

5. Calibrating & Reducing the Data

The data were recalibrated using the STSDAS task **calwp2**. A new dark reference file set was used for recalibration (j7r1737ku.r3h, j7r1737ku.b3h). All other recommended calibration reference files were used for recalibration.

The procedures outlined in WFPC2 ISR-95-04 (Whitmore and Heyer, July 1995) for performing aperture photometry were followed. The recommended IRAF/STSDAS scripts were modified for this data. Individual images were analyzed; images were not combined to remove cosmic rays due to small pointing offsets between the CR-SPLIT pairs. Identical stars were selected from the respective WF2, WF3, and WF4 frames. Stars were manually selected to avoid contamination from saturated star images, close or binary stars, cosmic rays mis-identified as stars, and for ease of cross-correlating photometry of star images from each frame.

Photometry was performed using the DAOPHOT task **phot** with the list of star positions manually identified as input. Aperture radius of 3.5 pixels was used with the sky annulus defined to be between 4 and 6 pixels. The centering algorithm was set to “centroid” with parameters cbox=3 and maxshif=1. All photometry values were written to tables for subsequent cross-correlation of identical targets in the WF2, WF3, and WF4 frames.

6. Preflashing Results

The amount of charge on the CCD chip, and thus available to fill traps, depends upon the lamp-on time. The 8450 flat field exposures were 30 seconds in the F555W filter, yielding approximately 2,000 counts on average to the wide field detectors (gain=7 e⁻/DN). Table 3 presents the mean counts in a region [100:800,100:800] for each chip.

Table 3. F555W Filter Flat Field Statistics (exp=30 sec.).

APERTURE	NPIX	MEAN	STDDEV	MIN	MAX
PC1	491401	409.	54.3	2.329	1648.
WF2	491401	2320.	280.8	4.597	3778.
WF3	491401	2235.	285.5	4.287	3785.
WF4	491401	1544.	255.8	1.697	3791.

The vignetted regions for each chip near the edges with adjacent chips were not used to determine the mean counts. The lamp-on exposure time was set to produce a maximum effect on the wide field chips. The PC1 aperture is not important for this report.

Figures 1-3 show comparisons of the “preflash ratio” (preflash/non-preflash) for the wide field chips (WF2, WF3, WF4). The preflash ratio is defined as the ratio between preflash and non-preflash measurements of the same star at the same location on the same chip. Y-preflash is defined as the percentage of ratio increase (slope) over 800 pixels in the Y direction. Except for the WF2 observations, the stars were imaged essentially at identical positions on the respective chips. Due to guide star problems, the star images moved approximately 5.6 pixels between the non-preflashed and preflashed WF2 observations. No corrections for CTE were applied. Photometry of stars of all intensities were used for the analysis. A few points outside of the range $0.9 < \text{Y-preflash} < 1.1$ (presumably due to cosmic ray, etc.) were discarded.

The mean value of Y-preflash increase is approximately $3.0 \pm 0.9\%$ for the wide field chips. Due to the limited number of stars and the number of observations, the chip-to-chip differences between the measured Y-preflash values on the different chips are not significant. From these plots it is apparent that the noiseless preflash increases the stellar counts at high CCD Y numbers by about 3%. At low CCD Y numbers there is no effect. This behavior is consistent with a reduction in the CTE photometry ramp.

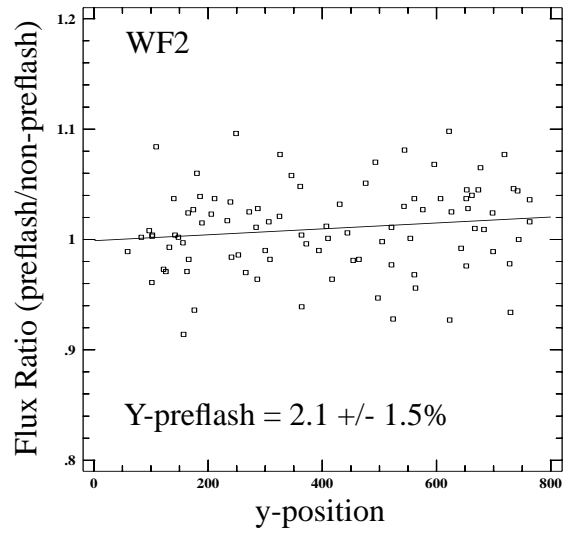


Figure 1: The ratio of the preflash/non-preflash flux in DN (u5ka010lr/u5ka010ir) vs. vertical position on the WF2 chip. The increase in % over 800 pixels (Y-preflash) is presented.

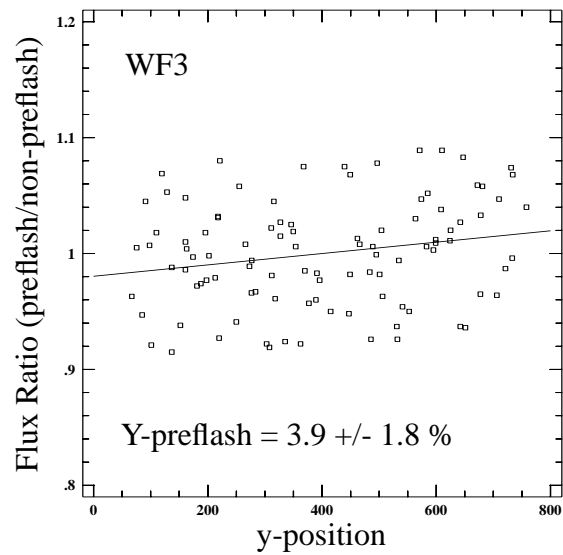


Figure 2: The ratio of the preflash/non-preflash flux in DN (u5ka010dr/u5ka010br) vs. vertical position on the WF3 chip. The increase in % over 800 pixels (Y-preflash) is presented.

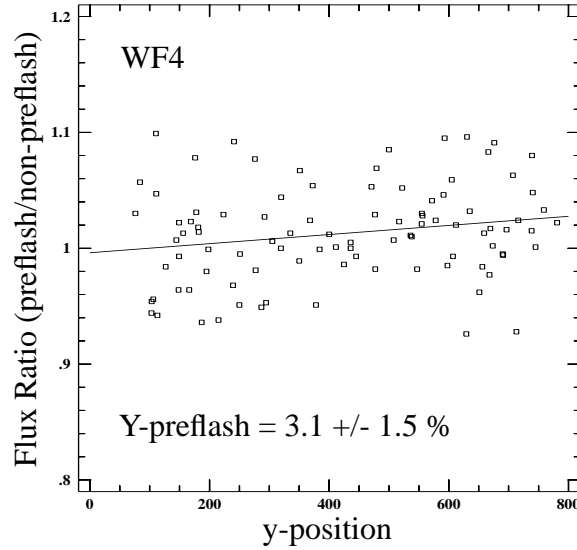


Figure 3: The ratio of the preflash/non-preflash flux in DN (u5ka0106r/u5ka0103r) vs. vertical position on the WF4 chip. The increase in % over 800 pixels (Y-preflash) is presented.

7. CTE Problem

Preflashing the CCD chips should minimize the CTE problem by filling the charge traps before an exposure. A comparison of the measured CTE for the non-preflash and preflash observations should indicate a decrease in the CTE loss. A decrease in the CTE loss would indicate that the majority of the charge remains in the traps longer than the time difference between the preflash and science exposures (approximately 2 minutes).

Figures 4-5 show the CTE measurements between apertures WF2 and WF4 before and after the preflash. Stars at the top of WF4 (Y=800) were found at the bottom of WF2 (Y=1). Hence, comparing the counts for a star on WF2 and WF4 provides a simple measure of CTE. Only stars with counts in the 3.5 pixel aperture in the range 100 to 500 DN are included in this analysis. The detected counts were corrected for X-CTE using formula (1b) from Whitmore, Heyer, and Casertano (1999), so as to isolate Y-CTE effects. A few points outside of the range $0.5 < \text{Flux Ratio} < 1.5$ were discarded and not used to determine the fit to the line. Presumably these points were affected by cosmic rays.

$$\text{X-CTE} = 2.5 * [1 + 0.341(0.00720 - 0.0020\log_{10}\text{CTS}_{\text{obs}})*(MJD - 49471)]$$

$$\text{CTS}_{\text{cor}} = [1 + \text{X-CTE}/100 * X/800] * \text{CTS}_{\text{obs}}$$

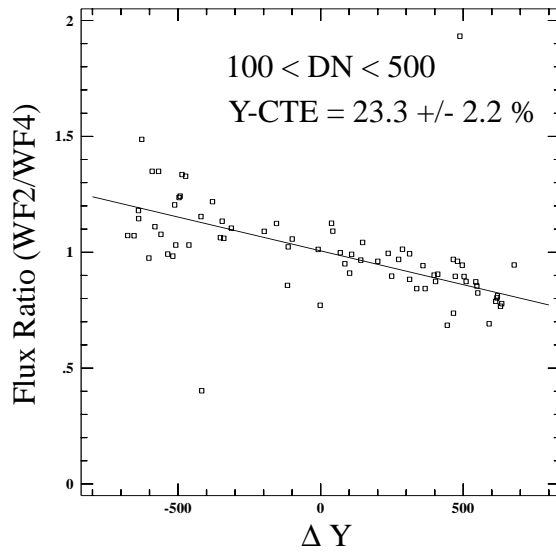


Figure 4: The detected flux ratio vs. ΔY for the F555W filter. The figure shows the data for WF2 vs. WF4 (u5ka010hr/u5ka0103r) with the Y-CTE loss in % over 800 pixels.

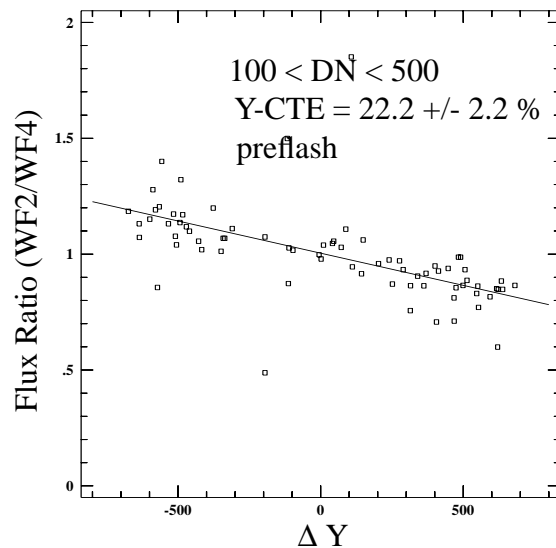


Figure 5: The detected flux ratio vs. ΔY for the F555W filter. The figure shows the pre-flash data for WF2 vs. WF4 (u5ka010kr/u5ka0106r) with the Y-CTE loss in % over 800 pixels.

The comparison between the non and preflash Y-CTE loss measurements (Figures 4 and 5) suggests that the preflash reduced the Y-CTE loss by $1.0 \pm 3.0\%$ over 800 pixels. The basic assumption is that electrons fill the traps and remain in the traps on a time scale long enough so that charge traps are not available to trap electrons in the targets as they are

read down a column. It appears that the majority of traps have time scales shorter than about 2 minutes which is the time difference between the start of the preflash exposure and the start time of the following observation.

8. Conclusions and Recommendations

The WFPC2 CCDs exhibit a less than ideal CTE. The CTE loss for faint stars on faint background has increased since 1995 from ~3% to as high as ~40% for a single faint star at the top of the chip (Y=800) (Whitmore 1998, Whitmore et al. 1999). Our preliminary results indicate, that at best, the noiseless preflash gives a modest decrease in the CTE effects. The noiseless preflash increased stellar counts at Y=800 by an average of 3.0 +/- 0.9%, while the measured Y-CTE loss was 8 times this amount. The improvement in the measured Y-CTE was 1.0 +/- 3.0%. It is evident from these results that the noiseless preflash electrons are not held in traps long enough to reduce the effects of CTE loss on aperture photometry of faint stellar targets.

To reduce the effects of CTE loss for faint, small targets, if possible, the target should be imaged close to the pyramid apex at pixel location (150,150). Closer than this position and one risks the target landing near the vignetted regions and affecting the resulting photometry. For wide field CCD chip imaging, aperture=WFALL is recommended. The WFALL aperture reference point is at pixel (133,149) on the WF3 chip. For the PC1 imaging, a POS TARG is needed to move the target from the reference point (420.0 424.5) to the desired (150,150) position (POS TARG -12.292, -12.491).

9. References

Biretta, J. and Mutchler, M. 1998, Charge Trapping and CTE Residual Images in the WFPC2 CCDs, WFPC2-ISR-97-05.

Casertano, S. and Mutchler, M. 1998, The long vs. short anomaly in WFPC2 images, WFPC2-ISR-98-02.

Clampin, M. 1992, WFPC-II CCDs, WFPC2-ISR-1992-06

Janesick, J. Soli, G., Elliott, T. and Collins, S. 1990, "Predicting the Effects of Proton Damage on Charge-Coupled Devices using the Radiation Transfer Technique", paper No. 103, IEEE 27th International Nuclear & Space Radiation Effects Conference, Reno, NV, July 16-20, 1990.

Whitmore, B and Heyer, I. 1995, A Demonstration Analysis Script for Performing Aperture Photometry, WFPC2 ISR-95-04.

Whitmore, B. and Heyer, I. 1998, New Results on Charge Transfer Efficiency and Constraints on Flat-Field Accuracy, WFPC2-ISR-97-08.

Whitmore, B. 1998, Time Dependence of the Charge Transfer Efficiency on the WFPC2, WFPC2-TIR-98-01.

Whitmore, B., Heyer, I., and Casertano, S. 1999, "Charge Transfer Efficiency of the Wide Field and Planetary Camera 2", PASP, 111, 1559-1576.